Renewable Energy 35 (2010) 1244–1254

Contents lists available at ScienceDirect

Renewable Energy

journal homepage: www.elsevier.com/locate/renene

California offshore wind energy potential

Michael J. Dvorak [a,*], Cristina L. Archer [b], Mark Z. Jacobson [a]

[a] Department of Civil and Environmental Engineering, Stanford University, Stanford, CA, USA
[b] Department of Geological and Environmental Sciences, California State University Chico, Chico, CA, USA

ARTICLE INFO

Article history:
Received 20 April 2009
Accepted 10 November 2009
Available online 9 December 2009

Keywords:
Offshore wind energy
California
Resource assessment
MM5
Bathymetry
Mesoscale modeling

ABSTRACT

This study combines multi-year mesoscale modeling results, validated using offshore buoys with high-resolution bathymetry to create a wind energy resource assessment for offshore California (CA). The siting of an offshore wind farm is limited by water depth, with shallow water being generally preferable economically. Acceptable depths for offshore wind farms are divided into three categories: ≤20 m depth for monopile turbine foundations, ≤50 m depth for multi-leg turbine foundations, and ≤200 m depth for deep water floating turbines. The CA coast was further divided into three logical areas for analysis: Northern, Central, and Southern CA. A mesoscale meteorological model was then used at high horizontal resolution (5 and 1.67 km) to calculate annual 80 m wind speeds (turbine hub height) for each area, based on the average of the seasonal months January, April, July, and October of 2005/2006 and the entirety of 2007 (12 months). A 5 MW offshore wind turbine was used to create a preliminary resource assessment for offshore CA. Each geographical region was then characterized by its coastal transmission access, water depth, wind turbine development potential, and average 80 m wind speed. Initial estimates show that 1.4–2.3 GW, 4.4–8.3 GW, and 52.8–64.9 GW of deliverable power could be harnessed from offshore CA using monopile, multi-leg, and floating turbine foundations, respectively. A single proposed wind farm near Cape Mendocino could deliver an average 800 MW of gross renewable power and reduce CA's current carbon emitting electricity generation 4% on an energy basis. Unlike most of California's land based wind farms which peak at night, the offshore winds near Cape Mendocino are consistently fast throughout the day and night during all four seasons.

1. Introduction

This paper quantifies the California (CA) offshore wind energy resource using three years of high-resolution mesoscale weather modeling data, locates shallow offshore areas where turbines could be erected using high-resolution bathymetry data, and calculates the overall energy and average power that could be obtained from offshore wind turbines. Wind power represents the fastest growing renewable energy resource, growing by 29% in 2008 alone to 120,798 MW of installed capacity worldwide. Offshore wind power grew at an even faster rate of 32% in 2008 with 1471 MW installed exclusively in the seas of Europe but still only represented 1.2% of the installed total worldwide [1].

Offshore wind turbines are subject to several additional constraints when compared to onshore wind turbines: (1) the cost of mounting the turbine to the sea floor is expensive and limited currently to shallow water depths, (2) undersea electrical transmission cable per unit distance is more expensive than overhead-land based transmission lines, (3) offshore weather and wave conditions can cause installation delays as rented equipment is forced to sit idle, and (4) maintenance costs of offshore turbines are higher. Although offshore wind turbines can be more costly to install and operate, they offer several distinct advantages over their onshore counterparts: (1) in general, they can be installed closer to coastal urban load centers, where most electrical energy demand exists, (2) transmission constraints and congestion are eased because offshore wind farms can be built closer to load centers, (3) offshore winds are faster and more consistent at lower vertical heights due to the reduced surface roughness over the ocean, and (4) offshore turbines and components are not limited by roadway shipping constraints, so higher capacity turbines can be installed. A detailed cost–benefit analysis between onshore and offshore wind has been performed [2], highlighting situations where offshore turbines installations are advantageous to onshore ones.

Although many offshore wind farms have been proposed in the US particularly off the US East Coast, no offshore turbines have been

* Corresponding author. Atmosphere/Energy Program, Jerry Yang & Akiko Yamasaki Environment & Energy Building – 4020, Stanford, CA 94305-4121, USA. Tel.: +1 650 454 5243; fax: +1 650 723 7058.
E-mail address: dvorak@stanford.edu (M.J. Dvorak).

0960-1481/$ – see front matter © 2009 Elsevier Ltd. All rights reserved.
doi:10.1016/j.renene.2009.11.022

installed as of 2009. Further, no sizable projects have been proposed on the US West Coast. The primary reason for the East Coast focus has been the significant area of shallow water suited for offshore turbine installation and highly concentrated coastal urban electric demand from Boston to Washington, D.C.

While onshore wind energy is a commercially viable choice for electricity generation, offshore wind turbines have the added constraint of being limited by the depth of water that the turbine can be installed in. In general, cost increases as the water depth increases. Current projects are limited to the relatively shallow waters, such as the continental shelves of Europe and the US East Coast. California waters in general become deeper than 20 m only a few km from shore, whereas waters off the East Coast remain as shallow as 20 m for tens of km offshore. The design of an offshore turbine foundation is a unique engineering problem for each specific wind farm, with loadings determined by winds, tides, and waves that are specific to that location in addition to geotechnical considerations. However, some generalizations can be drawn with respect to the foundation technology types used at different depths and the relative costs associated with these technologies.

Four general classes of offshore turbine foundations exist: gravity, monopile, multi-leg, and floating. In extremely shallow water (roughly 5 m depth) *gravity foundations* have been used [3]. *Monopile foundations* can be placed in waters up to approximately 20 m depth [3]. *Multi-leg foundations* designs that can be placed in waters up approximately 50 m depth have been successfully tested [4]. Floating turbine foundations are still in their prototype stage but will likely be developed in the coming years to unlock the vast deep water offshore wind resources around the world. These floating designs borrow heavily from existing oil and gas floating structure designs.

A general method to determine areas suitable for offshore wind production was developed by Dhanju et al. [5]. The methodology describes turbine foundation maximum depths of 20, 30, and 50 m for current monopile, future monopile, and multi-leg turbine foundations respectively and explores typical types of exclusions that prohibit turbines from being built in shipping lanes, avian flyways, and military zones. Because the methodology was developed in the relatively shallow water region of the East Coast, floating turbines were not considered. Floating turbines were considered however in an analysis of potential cost reductions of floating foundations over time [6]. The study provided an estimate of the California offshore wind resource based on bathymetry, distance from shore restrictions, and 50 m wind speed averages from AWS Truewind wind resource maps.[1]

After locations ideal for mounting offshore turbines have been identified, a wind resource assessment is performed in one of several ways. A simple method used for first order approximation is to scale existing long-term in-situ meteorological wind data from offshore buoys (typically at the 5 m height) [5] or satellite scatterometer wind data (e.g. NASA QuikSCAT as in Ref. [6]) up to the turbine hub height using the log law or power law for the vertical scaling of wind speed. These methods generally assume a neutrally buoyant boundary layer. Although the often long time series and high temporal resolution of the offshore buoys is important for climatological study, their spatial scope is limited. Scatterometer data can be useful for determining winds at low temporal and spatial resolution (e.g. QuikSCAT 0.5° horizontal and 6–24 h temporal resolution in Refs. [7] and [8]) but unfortunately may not be used for the coastal areas where land is present in the scatterometer swath. This limits QuikSCAT data to offshore areas farther out than approximately half the stated resolution of the data product. To the best of our knowledge, the highest horizontal resolution scatterometer wind data is 12.5 km [9].

An improved method to estimate 80 m wind speeds (modern turbine hub height) was developed that used local weather balloon soundings to determine the local surface roughness of the regional atmosphere [10]. Both of these methods rely on in-situ meteorological data, which is unfortunately sparse in the offshore CA region of interest. In order to model offshore winds, a mesoscale model can be employed and validated by the few offshore buoys that do exist. Mesoscale modeling has been found to be an appropriate method for studying offshore wind energy resource potential in several studies e.g. [11,12].

Several studies have looked at the meteorology of winds off the California coast e.g. [13–15]. The winds off the California coast are dominated mainly by two factors; the North Pacific subtropical high and the southwestern US thermal low [16]. The pressure gradient between these two surface pressure features and also the clockwise rotation of the Pacific High dominate the flow patterns off the California coast. The near surface winds are also highly influenced by the strong marine boundary layer (MBL) that forms due to the cold, coastal Pacific waters. This MBL surface inversion is strengthened in the spring and summer months, when surface winds flowing along the California coast enhance the upwelling of even colder water in the near coast region [17,18]. This strong MBL and prevailing northwesterly flow, usually at a height of around 500 m and with an inversion strength of 10 °C [19] traps winds at a height often lower than adjacent coastal topography, causing an increase in wind speed as the stream flows around capes and points along the coast. The highest wind speeds can often be found on the leeward side of these prominent capes and points, vertically bounded by the strong marine boundary layer, causing the flows to become supercritical under certain conditions and speed up on the leeward side of the topographic feature (e.g. Cape Mendocino and Point Arena).

One overall CA resource assessment has been performed to date [6] and one study has characterized the unique boundary layer flows that might impact energy production at two hypothetical wind farms for offshore CA [20]. Musial and Butterfield [6] found that significant resource potential existed off the coast of California in mostly deep waters. A global study of offshore surface wind power distributions using Quikscat Level-2 satellite wind measurements at 12.5 km horizontal resolution was also performed [21]. The study pointed out high average wind speeds on the leeward side of Cape Mendocino, CA but only in the deep water areas.

This study analyzes the California offshore wind energy potential at the modern wind turbine hub height of 80 m. No previous study has combined high horizontal resolution wind fields (5 and 1.67 km), high-resolution bathymetry data (~30 m), and the modern turbine hub height of 80 m in a wind resource assessment for offshore CA.

2. Method to determine the wind resource

To estimate the offshore wind resource, the basic steps performed were as follows. First, the areas over which offshore wind could be developed were determined using a bathymetry dataset and a geographical information system (GIS) (Section 2.1). Second, two mesoscale modeling domains that covered the areas of interest were created. Next, climatologically significant years based on the wind climatology of offshore buoy data were modeled (Section 2.2). These modeled years were validated using the offshore buoy data and the average wind resource at the turbine hub height (80 m) was calculated (Section 2.3). It was assumed that if the winds at the surface height were valid, the winds at the 80 m wind turbine hub height were also representative of the true wind resource. The wind resource derived in this section is used in Section 3 to estimate the offshore energy potential.

[1] The website for the wind resource maps is no longer available.

2.1. Offshore areas suitable for development

To estimate the wind resource potential based on depth, the bathymetry data were classified by each type of turbine foundation; 0–20 m for monopiles, 20–50 m for multi-leg, and 50–200 m for floating turbines. These depths are used as turbine foundation constraints throughout the study and coincide with the depths used in the offshore wind assessment methodology [5], with the exception that the 30 m "future" monopile class was ignored to simplify the study and remain consistent with general experience to date with monopile foundations (as reviewed in the Introduction). We have neglected gravity base turbine foundations, due to their limited utility in CA's generally deeper water. Deep water floating turbine foundations were considered for 50–200 m depth, similar to Ref. [6]. We only generalize depth classes here to roughly classify the potential cost and technological requirements of developing wind farms in shallow versus deep water.

The National Geophysical Data Center (NGDC) 3-arc second Coastal Relief Model [22] provided approximately 30 m horizontal resolution bathymetry for the offshore domain. In order to determine the amount of usable area for offshore wind turbines, the bathymetry map was divided into tower foundation classes (20, 50, and 200 m max depth) in a GIS. A map of the depth classes can be found in Fig. 1. The map has been subdivided and zoomed in on three geographical regions to clarify where shallow water areas exist. These three geographic areas, Northern (NCA), Central (CCA), and Southern (SCA) (see Fig. 1), are utilized later to give the wind resource context.

2.2. Mesoscale wind modeling

In order to estimate winds offshore, where little in-situ data exist, the Penn State/National Center for Atmospheric Research *Mesoscale Model version 5* (MM5) weather model [23] was run over the offshore parts of CA found suitable for turbine development in the previous section. The decision to use MM5 instead of in-situ data and/or satellite wind fields was based on the high spatial and temporal resolution wind fields that mesoscale modeling would provide. MM5 was run in nested mode with a parent and single nested domain configuration. Fig. 1 shows the domain configuration for MM5. The parent domain was run at 5.0 km horizontal resolution covering the entire on/offshore CA region. A higher resolution one-way-nested domain at 1.67 km horizontal resolution was created inside the CCA region. The nested domain was centered over the San Francisco Bay because this region contains the most concentrated shallow water areas (0–50 m) and the complex coastal mountain topography of the San Francisco Bay is not resolved well at the 5 km resolution. Compared to using the highest resolution QuikSCAT data available of 12.5 km horizontal resolution and 12 h temporal resolution [9], our 5.0 and 1.67 km resolution domains are roughly 6.25 and 56.0 times more spatially resolved respectively. The temporal resolution is also 12 times more resolved, as the SeaWinds/QuikSCAT satellite only passes over each offshore area twice per day.

One-way nested domains have been found to be appropriate for modeling offshore areas [11]. MM5 was configured with the Medium-Range Forecast (MRL) planetary boundary layer scheme, the Grell cumulus parameterization, and the Simple Ice (Dudhia) moisture scheme for the outer domain 1 and the mixed-phase (Reisner 1) moisture scheme for the nested domain 2 over the San Francisco Bay Area [23,24].

MM5 was run for the months of January, April, July, and October 2005/2006 (8 modeled months total) and the entirety of 2007 (12 months) to calculate seasonal and annual average wind speeds and average power density for the offshore wind resource. The National Center for Environmental Prediction 1° by 1° Global Final (FNL) Analyses were used to create initial and boundary conditions for MM5 in forecast mode [25]. Boundary conditions were updated every 6 h. The model was restarted every 7 days and reinitialized with the FNL data. Additionally, 6 h were added to each model run to allow the model to spin-up before the wind fields were used. The extra 6 h at the beginning of the forecast were discarded and not used in the calculation of the wind resource. The MM5 model was run using 8-128 processors on a GNU/Linux clusters at NASA Advanced Supercomputing Division and Stanford University.

In order to ensure that the modeled wind resource was reasonably climatologically significant, wind speeds from all available National Oceanic and Atmospheric Administration (NOAA) National Data Buoy Center (NDBC) offshore CA weather buoys from 1998 to 2008 were examined [26]. For this 11 year period, the mean 5 m wind speed and standard deviation (σ) were calculated from in-situ data for the 16 buoys shown in Fig. 2 and compared with the 11 year average. This 11 year period was assumed to be representative of the climatological average. The three years chosen (2005, 2006, 2007) had collective annual buoy mean wind speeds varying −7%, −3%, and 2% respectively from the mean. The annual σ varied −5%, 0, and 5% respectively from the mean σ. The years chosen may slightly underestimate the wind resource and hence make this estimate slightly conservative because of the model years chosen.

In order to more accurately resolve the average annual 80 m wind speed ($\overline{v}_{80\ \mathrm{m}}$), two additional horizontal layers (sigma-half levels) were added to the MM5 model directly above and below the 80 m offshore height, with a total vertical resolution of 28-levels full sigma-levels ($p_{\mathrm{top}} = 100$ hPa). Increased vertical resolution in MM5 was found to slightly increase the accuracy of wind prediction offshore [11]. The MM5 10 m wind speed was used to validate the modeled winds against 5 m offshore buoy wind data (next section). All of the wind data were inserted into a large, geospatial database based on PostGIS and PostgreSQL that allowed geospatial querying of the wind data underlain with the bathymetry data of different depth classes.

To reduce the amount of computer time needed for a climatologically significant wind resource study four seasonal months (Jan, Apr, Jul, and Oct) were modeled for two of the model years used in the study (2005 and 2006) instead of the entire 12 months. It was assumed that $\overline{v}_{80\ \mathrm{m}}$ of the four seasonal months approximated the $\overline{v}_{80\ \mathrm{m}}$ of the entire 12 months of that year. To assess the error that could potentially be introduced into the annual wind resource using this assumption, a comparison of $\overline{v}_{80\ \mathrm{m}}$ for the 12 months of 2007 was compared with $\overline{v}_{80\ \mathrm{m}}$ that only used the four seasonal months. The amount of energy produced in 2007 by the seasonal method was 1.6% higher (using the entire 0–200 m offshore zone) than that using all 12 months to estimate $\overline{v}_{80\ \mathrm{m}}$.[2] Interannual energy production variation differed by 50–76% going from the 2006 to the 2007 seasonally derived $\overline{v}_{80\ \mathrm{m}}$. This suggests that interannual variation plays a larger role in resource uncertainty than seasonal variation, emphasizing the importance of running multiple years of simulation versus one complete year, given the same amount of computing resource. Spatially, using the 12-month versus the seasonal method estimated slightly higher winds in NCA region ($\Delta\overline{v}_{80\ \mathrm{m}} = 0.43\ \mathrm{ms}^{-1}$, $\sigma = 0.12\ \mathrm{ms}^{-1}$), almost no variation in the CCA region ($\Delta\overline{v}_{80\ \mathrm{m}} = 0.11\ \mathrm{ms}^{-1}$, $\sigma = 0.10\ \mathrm{ms}^{-1}$), and slightly lower winds in the SCA region ($\Delta\overline{v}_{80\ \mathrm{m}} = 0.28\ \mathrm{ms}^{-1}$, $\sigma = 0.15\ \mathrm{ms}^{-1}$), where $\Delta\overline{v}_{80\ \mathrm{m}}$ was the mean difference in the $\overline{v}_{80\ \mathrm{m}}$ using 12-month minus the seasonal method.

Fig. 2 shows the weighted average of the modeled $\overline{v}_{80\ \mathrm{m}}$ and average wind power density for the months of January, April, July, and October 2005/2006 and the entirety of 2007. Using the weighted

[2] This corresponds to the installation of 45–80% more turbines. This increase is due to the difference in which offshore areas have the necessary cutoff speed of $\overline{v}_{80\ \mathrm{m}}$ of 7.0 and 7.5 ms^{-1} respectively. This energy resource calculation method is explained in detail in Section3.

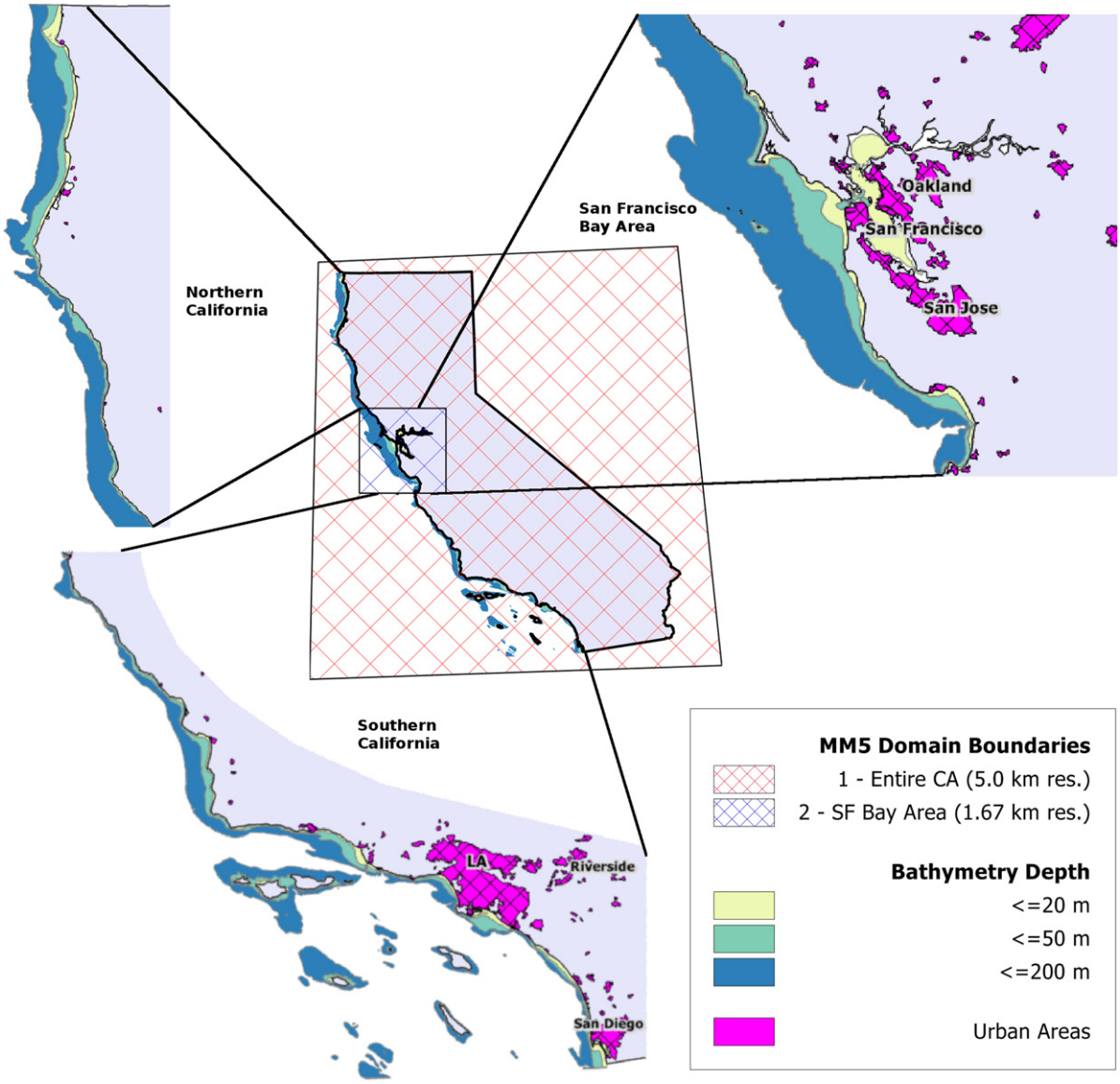

Fig. 1. California coastal bathymetry, based on foundation depth classes for monopile, multi-leg, and floating turbine foundations. Also shown are the MM5 parent and nested 1-way domain at 5 and 1.67 km respectively used for modeling the 80 m offshore wind resource.

average of these two seasonal years and one complete year of modeled data with hourly output, the annual $\overline{v}_{80\ \mathrm{m}}$ and average wind power density was predicted offshore.

2.3. Validation of modeling results

In order to validate the 10 m surface wind speeds obtained from the MM5 modeling, the 7-day MM5 model runs described above were compared with ocean-buoy mounted anemometers maintained by the *NOAA NDBC* [26]. Sixteen NDBC offshore buoys that fell within the MM5 course resolution modeling domain 1 were used to compare surface winds in the MM5 model (see Fig. 2 for a map of the buoy locations). MM5 10 m winds were plotted along side the 5 m buoy winds (Fig. 3), without correcting for the 5–10 m height difference. The plots in Fig. 3 give a representative group of MM5 domain 1 and 2 wind speeds along side the buoy data. In general, the MM5 winds show excellent agreement with the in-situ buoy data, as synoptic scale and diurnal winds were well matched.

Tables 1 and 2 show relevant error calculations between the buoy observations at 5 m and the MM5 domain 1 (5.0 km, see Fig. 1) 10 m wind speeds, including mean, standard deviation, root mean square error (RMSE), and bias. In order to adjust the 5 m buoy winds to the standard surface wind speed height of 10 m, the vertical wind profile log law was employed (assuming a neutral vertical temperature profile of the atmosphere). The log law surface roughness of $z = 0.0002$ was used to derive a 1.0684 multiplier to scale the 5 m buoy winds to the 10 m MM5 height [27].

A criterion for assessing the skill at which meteorological fields are predicted is given in [28]. These criteria are given as follows: (1) $\sigma \approx \sigma_{\mathrm{obs}}$, (2) $E < \sigma_{\mathrm{obs}}$, and (3) $E_{\mathrm{UB}} < \sigma_{\mathrm{obs}}$, where σ is the standard deviation of the modeled field, σ_{obs} is the standard deviation of the observation, E is the RMSE between the model and observations, and E_{UB} is the "bias corrected" RMSE, explained in [29]. Criteria (1), (2), and (3) above were met within reason for both domain 1 and 2 results for all months modeled, as can be verified in Tables 1 and 2.

Hourly $v_{80\ \mathrm{m}}$ winds were interpolated from vertical σ-layers of MM5. The median vertical wind speed profile log law surface roughness length (z) and power law friction coefficient were calculated by solving the log and power law equations for z and α. Using the domain 1 MM5 2007 hourly data from the 10 to 80 m height in

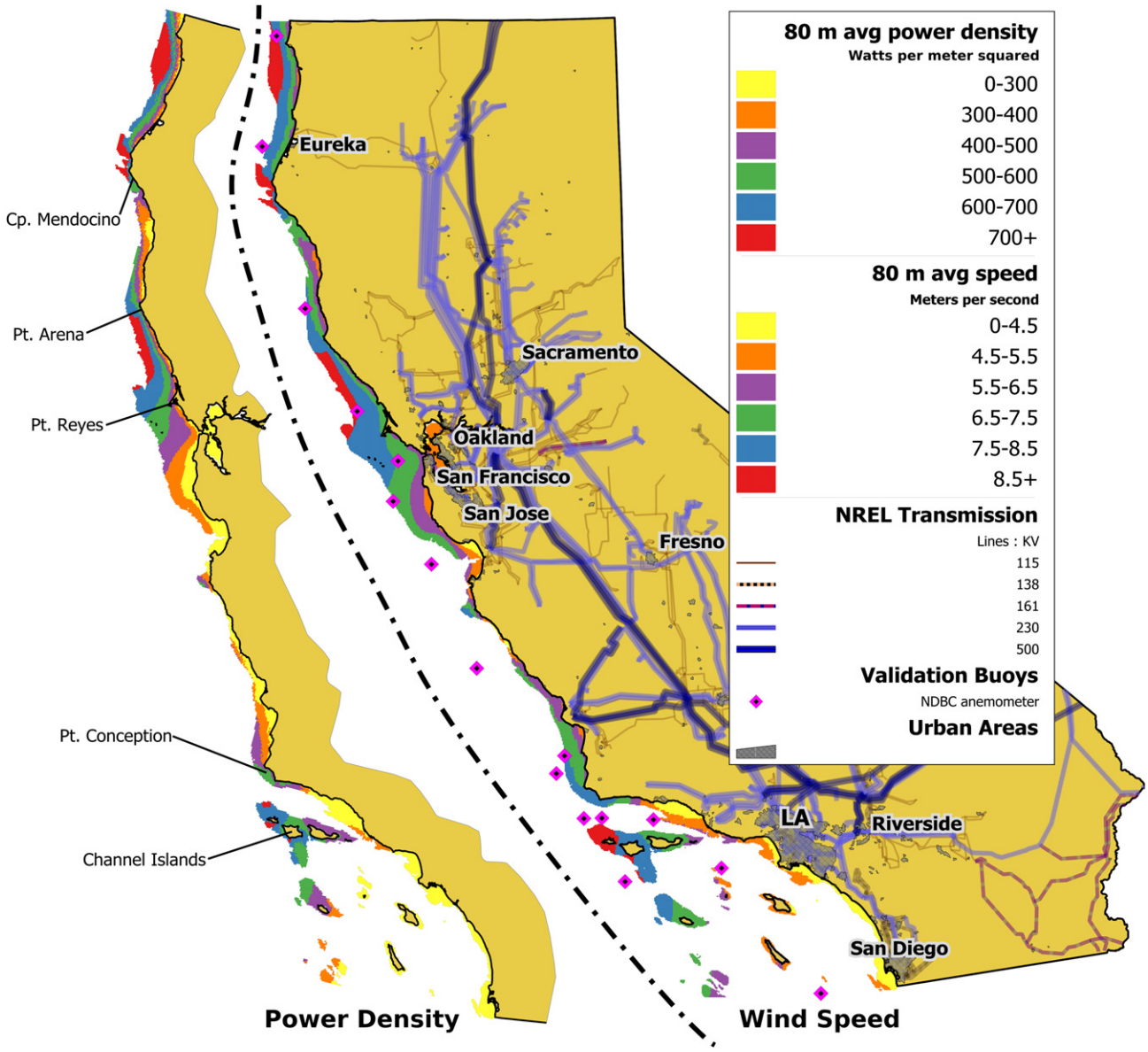

Fig. 2. Modeled 80 m average power density (left) and wind speed (right), based on seasonal 2005/2006 and complete 2007 MM5 winds. The wind resource corresponding to 0–200 m depth is shown. Locations where $\overline{v}_{80\,\mathrm{m}} \geq 7.5\ \mathrm{ms}^{-1}$ and $7.0\ \mathrm{ms}^{-1}$ were considered in this study. Urban areas highlight where the electricity demand exists. Transmission lines show where offshore wind farms could connect to the existing grid infrastructure.

the 0–200 m depth coastal California region, the median values for z and α were found to be 6.02E−4 m and 0.0732 respectively. Both of these coefficient values are expected over open water in neutral vertical temperature profile conditions [27].

Qualitatively, increased wind speeds on the leeward side of prominent capes like Cape Mendocino, Point Arena, and Point Conception are apparent in the Fig. 2. These modeling results were consistent with [13,20,30]. This suggests that MM5 was correctly predicting the MBL height relative to the adjacent coastal topography that is causing these supercritical channel flows. Additionally, strong coastal winds were predicted until south of Point Conception where much of coastal SCA is shielded by the CA Bight. At the Bight, the alongshore winds separate and continue far offshore. These modeling results are consistent with [13,16].

The San Francisco Bay (SFB) area winds however are likely to be under predicted due to the 1.67 km resolution nested domain not resolving the coastal mountain ranges. Gaps in the mountain ranges that can cause high winds to be channeled past the San Francisco International Airport and San Carlos Airport (KSQL) are only 1–2 km wide [31]. For example, the average July 2007 10 m winds at KSQL were underestimated by 68% by MM5, although σ was within 25%. This suggests that while the topography was not adequately resolved to accelerate the winds through the mountain gap, the diurnal wind variability was reasonably correct. The SFB $\overline{v}_{80\,\mathrm{m}}$ should be considered as not adequately resolved to detect these accelerated gap flow locations and warrants further research to locate potential high $\overline{v}_{80\,\mathrm{m}}$ areas.

3. Estimating energy production potential

This section uses the annual $\overline{v}_{80\,\mathrm{m}}$ calculated in Section 2 and combines it with depth classes for different types of turbine foundations (defined in Section 2.1) to calculate the wind energy resource for offshore CA. The surface areas of different depth classes are summed up and grouped by the geographical regions defined in Section 2.1. The annual $\overline{v}_{80\,\mathrm{m}}$ was calculated over each geographical

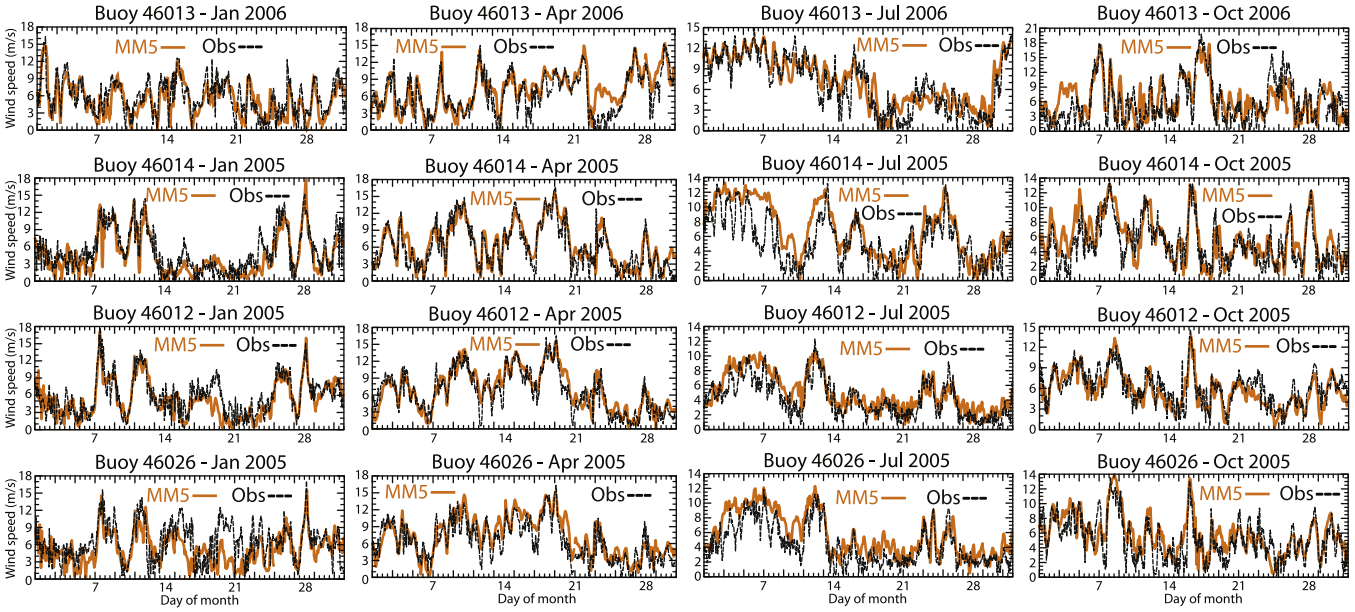

Fig. 3. 16-Months of representative 10 m height MM5 winds and the 5 m height NDBC buoy winds. The first two rows are from Domain 1 (5 km resolution, CA inclusive) and the last two rows are from Domain 2 (1.67 km resolution, San Francisco Bay Area). Buoy station number and year-month are indicated on each individual. See Fig. 2 for location of the NDBC buoys.

region and depth class. Specifications from a representative 5 MW offshore turbine were used to calculate how many turbines could be built in each region. These turbine specifications were also used to calculate the capacity factor (CF) over each region/depth class and annual energy/power estimates based on the annual $\overline{v}_{80\,\mathrm{m}}$ found in each region (Section 3.1). The regional implications of the offshore wind energy resource, based on transmission access and electricity demand are discussed in Section 3.2. Finally, the utility of an example wind farm in some of the best offshore wind resource and shallow water is shown (Section 3.3). Hourly power production of the wind farm is explored, to illustrate the potential usefulness of this resource.

3.1. Calculation of wind resource at different depths

Using the $\overline{v}_{80\,\mathrm{m}}$ calculated in Section 2, offshore areas where $\overline{v}_{80\,\mathrm{m}} \geq 7.5$ and 7.0 ms^{-1} were selected for potential turbine development. The 7.5 ms^{-1} cutoff was chosen to coincide with the National Renewable Energy Laboratory (NREL) *Class 5* resource, with a average power density of 500 $\mathrm{W/m}^2$ [32]. The 7.0 ms^{-1} cutoff was chosen to include the future possibility of an offshore wind turbine that could utilize lower wind speeds (NREL *Class 4*). The geospatial intersection of the NGDC bathymetry data and the annual modeled wind resource greater than 7.5 and 7.0 ms^{-1} is the basis for the surface areas in Table 3.

To simplify the offshore wind resource assessment, the average wind speeds were grouped by ocean depth and cutoff wind speed, shown in Table 3. In order to calculate annual energy production, it was necessary to pick a specific turbine model. The REpower 5M, 5 MW wind turbine with a 126 diameter at 80 m height was chosen [33]. Although the hub height for the offshore REpower 5M, is 90–100 m, this study used the slightly more conservative 80 m height. The wind speed would be approximately 1.7% faster at the 100 m height, based on the vertical wind profile log law ($z = 0.0002$) [27].

In order to determine how much water surface area would be required for each turbine, a 4-diameter by 7-diameter spacing [27] was chosen between turbines, where the turbine diameter is 126 m. Each REpower 5M turbine would require 0.44 km^2 of area per turbine. In order to account for the water surface area that would potentially be unusable due to shipping lanes, restricted wildlife preservation areas, viewshed considerations, etc., a 33% exclusionary factor for all possible turbine areas was included in each nameplate capacity and energy calculation. We used a 33% exclusionary factor in lieu of a complete exclusion zone assessment based on a study by Kempton et al. [34]. That study found that the sum of the avian flyways, waste areas, beach nourishment borrow areas, and shipping lanes was 35% of the available water area from 0 to 40 m and 10% at the 50–100 m depth waters, making our 33% exclusionary factor conservative for the mostly deep California offshore areas. Future studies should look at the details of each area's exclusion zones, in order to more precisely calculate amount of usable surface area. Table 4 shows the nameplate capacity of each geographical region and depth class.

The $\overline{v}_{80\,\mathrm{m}}$ calculated in the previous section was used to determine turbine CF, which in turn yielded an annual energy and average power output at each offshore site with suitable wind resource and shallow water. The CFs for the proposed wind farms were estimated using Eq. (1)

$$\text{Capacity Factor} = 0.087 \times V_{\mathrm{avg}}(\mathrm{m/s}) - \frac{P_{\mathrm{rated}}(\mathrm{kW})}{D^2(\mathrm{m})} \tag{1}$$

which states the relationship between mean wind speed (V_{avg}), rated power (P_{rated}) and rotor diameter (D) [27], using the turbine dimensions for the REpower 5M turbine. This equation has been shown to apply to a wide variety of wind turbine types [35] and was also utilized in three wind resource studies [20,35,36].

We have assumed a Rayleigh distribution over time of winds at the 80 m hub height by using the CF Eq. (1) explained in [27]. The error of using Eq. (1) to calculate CF was estimated by integrating the hourly power output from the REpower 5M turbine for all the MM5 model data from 2007 in the 0–200 m depth region. Using domain 1 (see Fig. 1) grid points where $\overline{v}_{80\,\mathrm{m}} \geq 7.5\ \mathrm{ms}^{-1}$ corresponding to NREL Class 5 winds (500–600 Wm^{-2}), the CF method

Table 1
Error calculations for the MM5 Domain 1 using the NDBC offshore buoys to ground truth the MM5 wind field data. (wt avg) is a time weighted average of the monthly statistic in that row.

Domain 1																								
Year	2005					2006					2007													
Month	Jan	Apr	Jul	Oct	(wt avg)	Jan	Apr	Jul	Oct	(wt avg)	Jan	Feb	Mar	Apr	May	Jun	Jul	Aug	Sep	Oct	Nov	Dec	(wt avg)
Avg mm5 (ms^{-1})	4.72	6.69	6.38	5.86	5.91	5.70	6.16	6.23	4.89	5.75	5.96	6.24	6.43	7.92	7.75	7.97	7.09	6.77	5.96	5.92	5.02	6.83	6.69
Avg buoy (ms^{-1})	5.69	6.88	5.32	5.58	5.85	6.22	6.22	6.03	4.75	5.80	6.24	6.76	6.62	7.96	6.95	7.15	6.71	6.24	5.24	5.82	5.16	7.18	6.53
Std dev mm5 (ms^{-1})	2.99	3.37	2.46	2.82	2.90	3.24	2.87	2.65	2.59	2.83	3.53	3.08	3.15	3.18	3.48	3.11	2.91	2.68	3.21	3.33	2.84	3.67	3.20
Std dev buoy (ms^{-1})	3.32	3.67	2.98	3.01	3.24	3.42	3.25	3.29	2.84	3.19	3.74	3.49	3.46	3.57	3.56	3.33	3.04	2.94	3.34	3.47	3.13	3.90	3.43
RMSE (ms^{-1})	2.52	2.03	2.40	2.30	2.31	2.47	2.09	2.54	2.37	2.36	2.60	2.08	2.07	2.09	2.84	2.42	2.45	2.22	2.48	2.39	2.45	2.40	2.39
$RMSE_{UB}$ (ms^{-1})	2.27	1.95	2.02	2.17	2.10	2.31	2.07	2.10	2.24	2.17	2.53	1.99	2.03	2.04	2.71	2.19	2.26	1.95	2.31	2.32	2.36	2.32	2.27
Bias (ms^{-1})	−0.98	−0.19	1.06	0.28	0.05	−0.52	−0.07	0.20	0.14	−0.05	−0.28	−0.52	−0.19	−0.04	0.81	0.82	0.38	0.52	0.72	0.10	−0.13	−0.35	0.16
Count	9552	9304	9659	10,363		8126	9766	9213	9129		9483	7269	8141	8890	9908	9569	9630	5393	8644	8340	8337	8865	

Table 2
Error calculations for the MM5 Domain 2 using the NDBC offshore buoys to ground truth the MM5 wind field data. (wt avg) is a time weighted average of the monthly statistic in that row.

Domain 2																								
Year	2005					2006					2007													
Month	Jan	Apr	Jul	Oct	(wt avg)	Jan	Apr	Jul	Oct	(wt avg)	Jan	Feb	Mar	Apr	May	Jun	Jul	Aug	Sep	Oct	Nov	Dec	(wt avg)
Avg mm5 (ms^{-1})	5.13	7.16	5.94	5.85	6.01	5.19	6.74	5.99	4.05	5.48	6.43	6.88	6.60	7.66	7.35	8.31	6.51	6.46	5.15	5.27	4.72	6.98	6.47
Avg buoy (ms^{-1})	6.51	7.37	5.17	6.17	6.29	5.83	6.76	6.34	4.17	5.77	6.60	7.27	6.77	7.98	6.76	8.01	6.66	6.48	5.01	5.64	5.38	7.19	6.60
Std dev mm5 (ms^{-1})	2.92	3.53	2.68	2.63	2.93	2.95	3.03	2.73	2.31	2.75	3.52	2.99	2.95	3.08	3.49	3.13	2.75	2.78	2.98	2.84	2.72	3.51	3.07
Std dev buoy (ms^{-1})	3.34	3.82	3.33	2.98	3.36	3.19	3.44	3.36	2.67	3.16	4.02	3.57	3.48	3.32	3.30	3.21	3.08	3.03	3.11	3.22	3.33	4.00	3.40
RMSE (ms^{-1})	2.92	1.82	1.95	1.94	2.16	2.23	2.04	1.90	2.01	2.05	2.45	2.05	1.91	1.87	2.73	2.13	2.01	2.00	1.97	2.02	2.33	2.24	2.15
$RMSE_{UB}$ (ms^{-1})	2.57	1.73	1.76	1.87	1.98	2.12	2.03	1.83	1.98	1.99	2.42	1.99	1.87	1.79	2.63	2.01	1.89	1.95	1.92	1.96	2.20	2.22	2.08
Bias (ms^{-1})	−1.38	−0.21	0.77	−0.32	−0.28	−0.65	−0.02	−0.35	−0.12	−0.29	−0.18	−0.40	−0.17	−0.32	0.59	0.30	−0.15	−0.03	0.14	−0.37	−0.66	−0.21	−0.13
Count	2932	2837	2950	2947		2943	2822	2944	2911		2882	1979	1860	2080	2196	2650	2799	1714	2648	2892	2805	2930	

Table 3
Summary of usable bathymetry and the average wind speed composed of the January, April, July, and October 2005/2006 and 2007 (12 months) modeled MM5 data at the three different California regions. Only areas that had wind speeds higher than 7.0 ms^{-1} and 7.5 ms^{-1} at 80 m were included in this study.

Water depth	Cutoff	Northern CA		Central CA		Southern CA		Total	Area wt avg
	Speed (ms^{-1})	Area (km^2)	Speed (ms^{-1})	Area (km^2)	Speed (ms^{-1})	Area (km^2)	Speed (ms^{-1})	Area (km2)	Speed (ms^{-1})
0–20 m	≥7.0	171	7.68	29	7.26	242	7.82	442	7.73
	≥7.5	95	8.03	4	7.58	166	8.10	265	8.07
	Total	636		1285		1473		3394	
20–50 m	≥7.0	740	7.69	408	7.25	494	7.87	1642	7.63
	≥7.5	399	8.06	56	7.70	368	8.10	823	8.05
	Total	1513		1504		2438		5455	
50–200 m	≥7.0	4129	8.26	4313	7.96	3727	7.84	12,169	8.03
	≥7.5	3672	8.38	3400	8.13	2618	8.10	9690	8.22
	Total	5272		6639		8423		20,334	

on average *underestimated* the 2007 annual turbine energy output by 2.0% with 1st and 3rd quartiles of 0.5% and 3.5% respectively. This relatively small error is acceptable for the amount of utility the CF equation provides in allowing other turbine specifications to be used with the average wind speeds found in Fig. 2.

Using the $\overline{v}_{80\ m}$ for each depth class and wind cutoff from Table 3, the CF for each turbine foundation technology was calculated. Combining the CF calculation and the usable area (including the 33% exclusionary factor, Table 4), an annual energy estimate has been made in Table 5.

A significant amount of offshore wind energy potential does exist in California with 513–661 TWh (59–76 GW average) developable annually in all waters (see Table 5 for details). The range of energy production and average given is using the 7.5 and 7.0 ms^{-1} $\overline{v}_{80\ m}$ cutoff. While the vast majority (about 90%) of the California offshore wind resource exists in deep waters (50–200 m), a significant potential 51–93 TWh (6–11 GW average) exists in the shallower water regions that could be developed with current technology (0–50 m). The regional context of the resource including proximity to urban load centers and transmission lines is analyzed in detail in the following section.

3.2. Regional implications of the resource

In order to provide geographical context for the California offshore wind resource, we mapped the annual $\overline{v}_{80\ m}$ and average power density calculated in this study out to 200 m depth, transmission lines [37], and urban areas [38] in Fig. 2 for CA. By combining the modeled wind resource, annual energy output estimate with the more conservative 7.5 ms^{-1} $\overline{v}_{80\ m}$ cutoff (Table 5), and the transmission/depth maps, the feasibility for developing offshore wind along the coast in California was assessed in the three geographical regions.

NCA (Fig. 1) could potentially provide 12.3–19.7 TWh (1.4–2.2 GW average output) of wind energy annually in relatively shallow water (0–50 m), using existing turbine foundation technology. This amount of energy alone could offset 7–11% of CA's current carbon emitting electricity sources, based on the sum of all in and out of state electricity generation using coal, natural gas, and biomass, which was 174.746 TWh in 2006 [39]. Further, if deep water turbine support technology were developed, 114–235% of CA's current carbon electricity sources could be replaced by offshore wind energy in NCA alone.

The initial assessment for CCA (Fig. 1) looks less viable for near term development. The high $\overline{v}_{80\ m}$ seems to occur far from the city of San Francisco and exists primarily in deep waters (50–200 m, see Table 3 and Fig. 2 for details). As previously mentioned in Section 2.2, the coastal mountains of the San Francisco Bay (SFB) were not resolved highly enough in MM5 to recreate the mountain gap flows, where higher wind speeds are found. Most of the large transmission lines would need to be accessed through the San Francisco Bay inlet, as little coastal transmission access exists in the area (Fig. 2). One potentially interesting location in CCA is the Farallon Islands (managed by the City and County of San Francisco), which appear to have the necessary wind resource ($\overline{v}_{80\ m} \geq 7.5\ ms^{-1}$) and are surrounded by fairly shallow water (≤50 m depth). However, the length of undersea transmission cable required would be a lengthy 43 km. Further, the Islands' unique bird nesting, marine mammal, and fish populations would need careful review before turbines could be sited near this location. A positive attribute of the Islands' far distance from shore is that it would make the offshore wind turbines nearly impossible to see from San Francisco and might quell any viewshed concerns from City residents.

Based on our initial assessment, SCA (Fig. 1) appears to have little easily developable offshore wind resource. Much of the good wind resource exists about 50 km offshore, off Point Conception (see Fig. 2) and to the west of San Miguel Island and Santa Rosa Island (the

Table 4
Nameplate capacity of turbines (MW) in each geographical area, depth, and wind speed cutoff, assuming a 33% exclusionary factor for each area.

Water depth	Cutoff speed (ms^{-1})	Nameplate capacity (MW)			Total (MW)
		Northern CA	Central CA	Southern CA	
0–20 m	≥7.0	1289	219	1824	3331
	≥7.5	716	30	1251	1997
20–50 m	≥7.0	5577	3075	3723	12,374
	≥7.5	3007	422	2773	6202
50–200 m	≥7.0	31,116	32,503	28,087	91,707
	≥7.5	27,672	25,623	19,729	73,025

Table 5
Annual delivered energy (TWh) and average power (GW) in each geographical region, depth class, and cutoff wind speed. A 33% exclusionary factor was included in these calculations. These data correspond to the conditions outlined in Table 3.

Water depth	Cutoff speed (ms^{-1})	Annual delivered energy (TWh)			Total (TWh)	Avg. pwr. (GW)
		Northern CA	Central CA	Southern CA		
0–20 m	≥7.0	7.5	1.3	10.9	19.7	2.2
	≥7.5	4.4	0.2	7.7	12.3	1.4
20–50 m	≥7.0	32.7	18.0	22.3	73.0	8.3
	≥7.5	18.5	2.6	17.1	38.2	4.4
50–200 m	≥7.0	195.9	204.6	167.8	568.3	64.9
	≥7.5	176.7	163.6	121.8	462.1	52.8
Total	≥7.0	236.1	223.9	201.0	661.0	75.5
	≥7.5	199.6	166.4	146.6	512.6	58.5

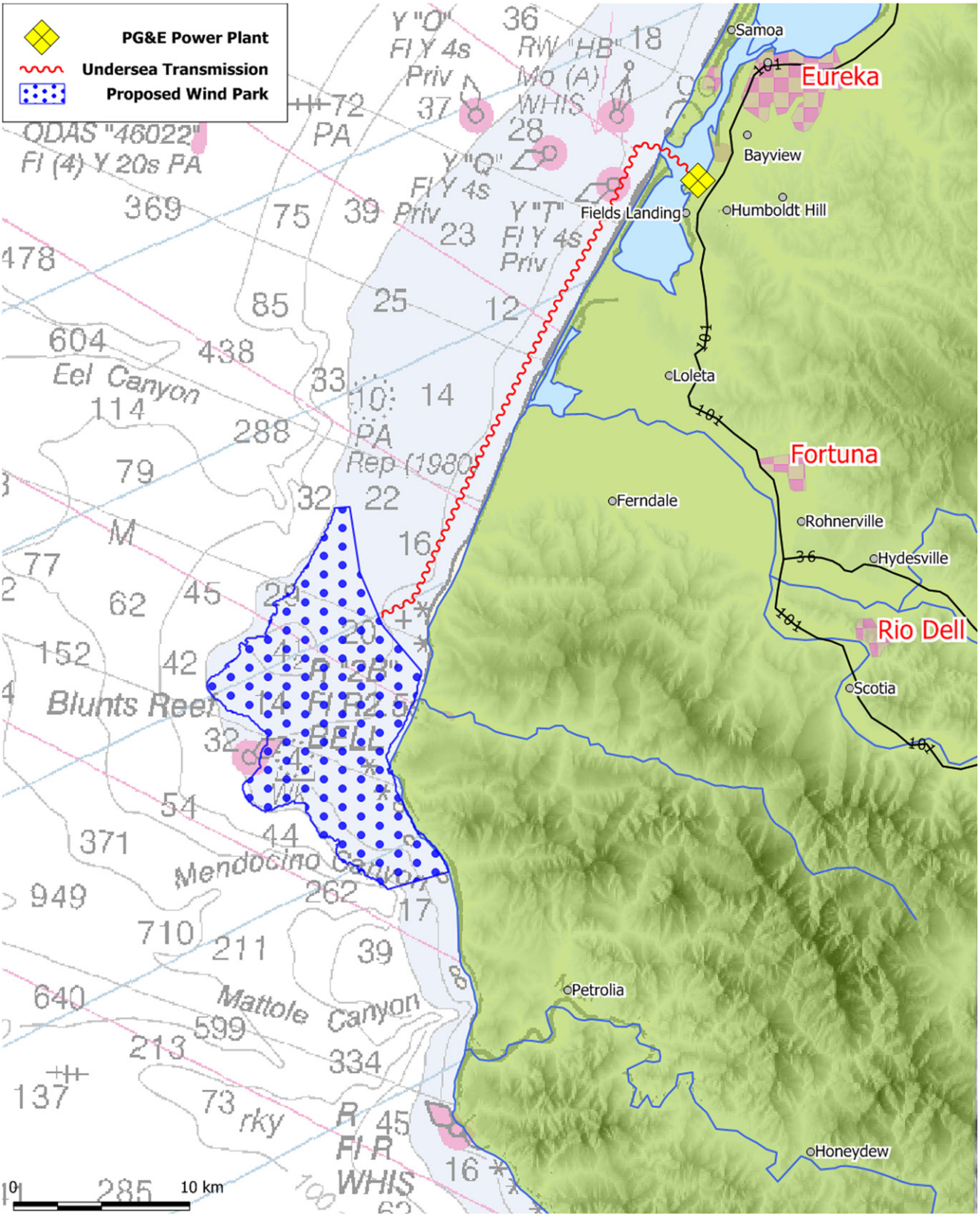

Fig. 4. A proposed wind farm off the Coast of Cape Mendocino located in water shallow enough for multi-leg turbine foundations (≤50 m) and having annual $\overline{v}_{80\,\mathrm{m}} \geq 7.5\ \mathrm{ms}^{-1}$ (based on the 2005/2006 model data). An undersea transmission cable would connect the wind farm to an existing power plant location in Humboldt Bay.

Channel Islands). Winds south and east of Point Conception are significantly reduced. Although alongshore coastal winds flow strongly until Point Conception, much of SCA is shielded by the CA Bight, where the alongshore winds separate and continue far offshore, leaving the Los Angeles area with little coastal wind. It should be noted however that the SCA coast does provide several excellent grid interconnection points and significant electrical demand.

3.3. Example offshore wind farm

To illustrate the possible utility that an offshore wind farm could provide to the California grid, an example offshore wind farm was created, located off Cape Mendocino (see map in Fig. 4). The proposed wind farm is located in water ≤50 m deep and could be developed today with existing turbine foundation technologies. Eureka is an idea location for this project because some existing (albeit small) 115 kV power lines cross the coastal mountains eastward to the main transmission corridor in the California central valley. Additionally, an existing power plant in Humboldt Bay would provide an ideal location to connect the sea transmission to the local electric grid.

The annual $\overline{v}_{80\ m}$ calculated using the January, April, July, and October 2005/2006 80 m wind speeds from MM5 (8 modeled months total) was 8.23 ms^{-1}, which corresponds to a 40% CF using Eq. (1) with the REpower 5M turbine. The wind farm would be most active however during the summer months, when the average 80 m wind speed calculated from the July 2005 and 2006 MM5 data is 9.67 ms^{-1}; a 53% CF during the summer months using Eq. (1) with the REpower 5M turbine.

The time of day when wind power peaks is important because the summer peak electric demand occurs late in the afternoon, around 5:00 pm [40]. Electricity generated during peak demand periods is more valuable than electricity generated during off peak periods, both for air pollution emissions reductions and monetary value. In order to analyze how offshore wind power might fit into the California electric grid, $\overline{v}_{80\ m}$ winds were averaged by hour over the eight seasonal months of the 2005/2006 MM5 model data and shown in Fig. 5. The summertime winds, denoted by the "July" line in Fig. 5 are fast and consistent throughout the day. These summer winds would dovetail extremely well with California electricity demand during the summer months. Unlike most California land based wind farms which peak at night, the offshore winds off Cape Mendocino are consistent throughout the day during the summer months [24].

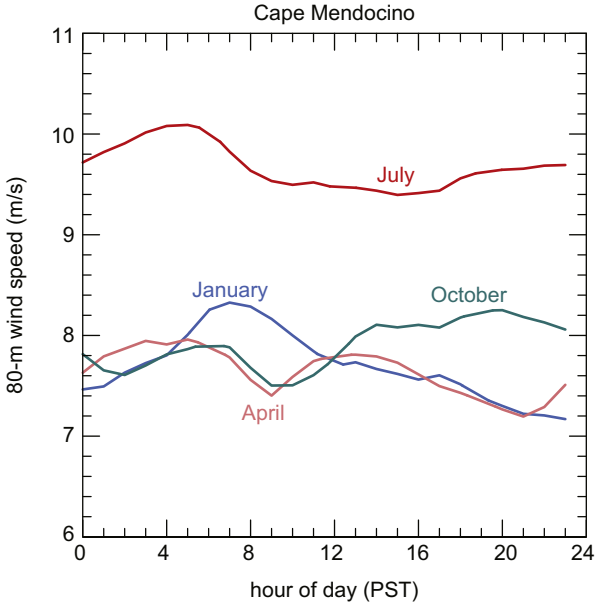

Fig. 5. Mean $\overline{v}_{80\ m}$ winds group by hour of the day (PST) for the proposed wind farm off the NCA coast (Fig. 4), based on the MM5 output for the 2005/2006 months of January, April, July, and October.

The proposed Cape Mendocino wind farm is 138 km^2 and could accommodate approximately 300 REpower 5M 5.0 MW wind turbines, with a total project rated capacity of 1500 MW (using a 4-diameter by 7-diameter turbine spacing, as well as a 33% exclusionary factor). The clean energy contribution of this wind farm would be quite significant in cleaning California's electricity supply. The annual energy output from this project alone could be 6.91 TWh annually, corresponding to an average power output of 790 MW. This wind farm alone could replace 4.0% (gross) of California's current carbon emitting electric generation (using the carbon emitting electricity generation from in and out of state resources of 174.746 TWh in 2006 from [39]).

4. Conclusions

Despite the steep bathymetry off the California (CA) coast, significant development potential exists for offshore wind energy. By looking at the depth of the water more closely, with a higher resolution bathymetry dataset, it was possible to find some areas that were previously overlooked for offshore wind power development. This study also qualitatively looked at transmission capacity and population centers to build a context for the offshore wind resource in CA. It was found that Northern California (NCA) had the best 80 m wind resource but the least transmission capacity compared to other parts of the state. Some NCA's resource could be developed today, using existing turbine foundation technology.

Central California will likely require the development of floating turbines for large scale offshore wind development. Some shallow water area (≤50 m) with good wind resource potential does exist near the Farallon Islands however. The relatively shallow San Francisco Bay was not resolved highly enough in the mesoscale model to draw conclusive results and warrants further investigation.

The Southern California (SCA) region will more than likely require the development of floating turbines for large scale offshore turbine development. Most of the viable wind resource exists far offshore in deep water and would require lengthy undersea transmission lines.

In sum, including all current and future turbine foundation technologies (0–200 m depth), based on the $\overline{v}_{80\ m}$ wind speed cutoffs of 7.5 ms^{-1} and 7.0 ms^{-1} between 174% and 224% respectively of CA electricity needs (including in-state plus imported generation, 294.865 TWh in 2006) could be provided with offshore wind energy alone [39]. Using only currently available turbine tower support technologies (0–50 m depth), between 17% and 31% respectively of CA electricity need could be provided.

An example wind farm was proposed near Cape Mendocino and the city of Eureka in water shallow enough to develop offshore wind turbines with existing turbine foundation technology. This 1500 MW, 300 turbine wind farm located in some of the best California offshore wind resource could replace up to 4.0% of its current carbon emitting electricity generation sources and would deliver nearly 800 MW of deliverable renewable power on average. Unlike most of California land based wind farms which peak at night, the offshore winds near Cape Mendocino are consistently fast during day and night for all four seasons.

Acknowledgments

We would like to thank (in alphabetical order) James Doyle, Crystal Dvorak, Jeffery Greenblatt, Tracy Haack, Nick Jenkins, Qingfang Jiang, Willett Kempton, Martin Ralph, and Zachary Westgate for

helpful comments. We would also like to thank John Taylor, for assistance with the MM5 modeling. Thank you to the National Aeronautics and Space Administration (NASA) *Advanced Supercomputing (NAS) Division* and National Center for Atmospheric Research's (NCAR) *Computational & Information Systems Laboratory (CISL)* for access to computational resources and global weather datasets respectively, used in the mesoscale modeling. Support for this work came from NASA, the Charles H. Leavell Fellowship, and Precourt Energy Efficiency Center.

References

[1] Global Wind Energy Council. Global wind 2008 report. Available from: http://www.gwec.net/fileadmin/documents/Publications/Report_2008/Global_Wind_2008_Report.pdf; 2009.
[2] Snyder B, Kaiser MJ. Ecological and economic cost–benefit analysis of offshore wind energy. Renewable Energy 2009;34:1567–78.
[3] Henderson AR, Morgan C, Smith B, Sorensen HC, Barthelmie RJ, Boesmans B. Offshore wind energy in Europe – a review of the state-of-the-art. Wind Energy 2003;6:35–52.
[4] Talisman Energy. Beatrice wind farm demonstrator project. Available from: http://www.beatricewind.co.uk/Uploads/Downloads/BEATRICE_WINDFARM.pdf; 2006 [accessed 24.01.07].
[5] Dhanju A, Whitaker P, Kempton W. Assessing offshore wind resources: an accessible methodology. Renew Energy 2008;33:55–64.
[6] Musial W, Butterfield S. Future for offshore wind energy in the United States. In: Proc. of EnergyOcean 2004. Available from: http://www.nrel.gov/docs/fy04osti/36313.pdf; 2004.
[7] Sørensen B. A new method for estimating off-shore wind potentials. International Journal of Green Energy 2008;5:139–47.
[8] Pimenta F, Kempton W, Garvine R. Combining meteorological stations and satellite data to evaluate the offshore wind power resource of Southeastern Brazil. Renewable Energy 2008;33:2375–87.
[9] Jet Propulsion Laboratory. Available from: QuikSCAT science data product user's manual, D-18053-Rev A. Available from: ftp://podaac.jpl.nasa.gov/ocean_wind/quikscat/L2B12/doc/QSUG_v3.pdf; 2006.
[10] Archer CL, Jacobson MZ. Spatial and temporal distributions of U.S. winds and wind power at 80 m derived from measurements. Journal of Geophysical Research 2003;108:4289.
[11] Beran J, Claveri L, Lange B, von Bremen L. Offshore wind modelling and forecast. In: Proc. of the 6th WRF/15th MM5 users' workshop. Available from: http://www.mmm.ucar.edu/wrf/users/workshops/WS2005/abstracts/Session3/30-Beran.pdf; 2005.
[12] Jimenez B, Durante F, Lange B, Kreutzer T, Tambke J. Offshore wind resource assessment with WAsP and MM5: comparative study for the German Bight. Wind Energy 2007;10:121–34.
[13] Dorman C, Winant C. Buoy observations of the atmosphere along the west coast of the United States, 1981–1990. Journal of Geophysical Research 1995;100:16029.
[14] Archer CL, Jacobson MZ, Ludwig FL. The Santa Cruz eddy. Part I: observations and statistics. Monthly Weather Review 2005;133:767.
[15] Haack T, Burk SD, Hodur RM. U.S. west coast surface heat fluxes, wind stress, and wind stress curl from a mesoscale model. Monthly Weather Review 2005;133:3202–16.
[16] Halliwell GR. The large-scale coastal wind field along the west coast of North America 1981–1982. Journal of Geophysical Research 1987;92:1861.
[17] Beardsley RC. Local atmospheric forcing during the coastal ocean dynamics experiment 1. A description of the marine boundary layer and atmospheric conditions over a northern California upwelling region. Journal of Geophysical Research 1987;92:1467.
[18] Taylor SV, Cayan DR, Graham NE, Georgakakos KP. Northerly surface winds over the eastern North Pacific Ocean in spring and summer. Journal of Geophysical Research 2008;113:D02110.
[19] Ralph FM, Neiman PJ, Persson POG, Bane JM, Cancillo ML, Wilczak JM, et al. Kelvin waves and internal bores in the marine boundary layer inversion and their relationship to coastally trapped wind reversals. Monthly Weather Review 2000;128:283–300.
[20] Jiang Q, Doyle JD, Haack T, Dvorak MJ, Archer CL, Jacobson MZ. Exploring wind energy potential off the California coast. Geophysical Research Letters 2008;35:L20819.
[21] Liu WT, Tang W, Xie X. Wind power distribution over the ocean. Geophysical Research Letters 2008;35.
[22] National Oceanographic and Atmospheric Administration, National Geophysical Data Center. National geophysical data center coastal relief model, 3-arc second. Available from: http://www.ngdc.noaa.gov/mgg/coastal/coastal.html; 2000.
[23] Grell GA, Dudhia J, Stauffer DR. A description of the fifth-generation Penn State/NCAR mesoscale model (MM5); 1994. p. 117.
[24] Fripp M, Wiser R. Analyzing the effects of temporal wind patterns on the value of wind-generated electricity at different sites in California and the Northwest, LBNL-60152; 2006.
[25] National Center for Environmental Prediction. NCEP global tropospheric analyses, 1 × 1, daily 15 Sep 1999–present (ds083.2); 2007.
[26] National Oceanic and Atmospheric Administration, National Data Buoy Center; 2008.
[27] Masters GM. Renewable and efficient electric power systems. Hoboken, NJ: John Wiley & Sons; 2004.
[28] Pielke Sr RA. Mesoscale meteorological modeling. San Diego: Academic Press; 2002.
[29] Keyser D, Anthes RA. The applicability of a mixed-layer model of the planetary boundary layer to real-data forecasting. Monthly Weather Review 1977;105:1351–71.
[30] Winant CD, Dorman CE, Friehe CA, Beardsley RC. The marine layer off Northern California: an example of supercritical channel flow. Journal of the Atmospheric Sciences 1988;45:3588–605.
[31] Gilliam H. Weather of the San Francisco Bay region. Berkeley: University of California Press; 2002.
[32] Elliot D, Schwartz M. Development and validation of high-resolution state wind resource maps for the United States. NREL/TP-500-38127. Available from: http://www.nrel.gov/docs/fy05osti/38127.pdf; 2005.
[33] REpower Sytems AG. REpower systems AG: 5 M goes offshore: the countdown is running. Available from: http://www.repower.de/index.php?id=369&L=1; 2007 [accessed 15.06.07].
[34] Kempton W, Archer CL, Dhanju A, Garvine RW, Jacobson MZ. Large CO_2 reductions via offshore wind power matched to inherent storage in energy end-uses. Geophysical Research Letters 2007;34:2817.
[35] Archer CL, Jacobson MZ. Evaluation of global wind power. Journal of Geophysical Research 2005;110:1.
[36] Yue C, Yang M. Exploring the potential of wind energy for a coastal state. Energy Policy 2009;37:3925–40.
[37] Federal Emergency Management Agency. Transmission lines for conterminous United States (115 kV and above). Distributed by the National Renewable Energy Laboratory. Available from: http://www.nrel.gov/gis/data_analysis.html; 1993.
[38] U.S. Geological Survey. Urban areas of the United States. Available from: http://nationalatlas.gov/mld/urbanap.html; 2001.
[39] California Energy Commission. 2006 Net system power report. Available from: http://www.energy.ca.gov/2007publications/CEC-300-2007-007/CEC-300-2007-007.PDF; 2007 [accessed 22.10.09].
[40] Price H, Cable R. Parabolic trough power for the California competitive market. Available from: http://www.p2pays.org/ref/18/17978.pdf; 2001.